Synthesis and Characterization of Wholly Aromatic Poly(azomethine)s Containing Donor–Acceptor Triphenylamine Moieties

GUEY-SHENG LIOU, HUNG-YI LIN, YU-LUN HSIEH, YI-LUNG YANG

Functional Polymeric Materials Research Laboratory, Department of Applied Chemistry, National Chi Nan University, Puli, Nantou Hsien 54561, Taiwan, People's Republic of China

Received 28 April 2007; accepted 20 May 2007
DOI: 10.1002/pola.22228
Published online in Wiley InterScience (www.interscience.wiley.com).

ABSTRACT: *N*-(4-nitrophenyl)-4′,4″-bisformyl-diphenylamine was synthesized from *N*-(4-nitrophenyl)-diphenylamine by the Vilsmeier-Haack reaction. Soluble aromatic poly(azomethine)s (PAMs) were prepared by the solution polycondensation of *N*-(4-nitrophenyl)-4′,4″-bisformyl-diphenylamine and aromatic diamine in *N*-methyl-2-pyrrolidone (NMP) at room temperature under reduced pressure. All the PAMs are highly soluble in various organic solvents, such as *N,N*-dimethylacetamide (DMAc), chloroform ($CHCl_3$), and tetrahydrofuran (THF). Differential scanning calorimetry (DSC) indicated that these PAMs had glass-transition temperatures (T_gs) in the range of 170–230 °C, and a 10% weight-loss temperatures in excess of 490 °C with char yield at 800 °C in nitrogen higher than 60%. These PAMs in NMP solution showed UV-Vis charge-transfer (CT) absorption at 405–421 nm and photoluminescence peaks around 462–466 nm with fluorescence quantum efficiency (Φ_F) 0.10–0.99%. The highest occupied molecular orbital (HOMO) and lowest unoccupied molecular orbital (LUMO) energy levels of these PAMs can be determined from cyclic voltammograms as 4.86–5.43 and 3.31–3.34 eV, respectively. © 2007 Wiley Periodicals, Inc. J Polym Sci Part A: Polym Chem 45: 4921–4932, 2007

Keywords: charge transfer; electrochemistry; functionalization of polymers; high performance polymers; polycondensation

INTRODUCTION

Poly(azomethine)s (PAMs), or poly(Schiff-base)s, with aromatic backbones are attractive high performance conducting polymers[1] due to their high thermal stability,[2] excellent mechanical strength,[3] and good optoelectronic properties.[4,5] Chen et al. reported the theoretical analysis on the geometries and electronic properties of various conjugated PAMs.[6–8] In recent years, PAMs have also been explored for applications in organic electronics, such as light-emitting diodes,[9] pH sensors,[10] and metal-collecting sites.[11,12] However, their insolubility in common organic solvents limits their processability and characterization.[13,14] The targeted PAMs therefore often bear large alkyl, alkoxy, or aryloxy groups to improve solubility, thus lower their glass transition temperatures (T_gs) and thermal stability. Over the past 25 years, different methods have been adopted toward processable PAMs by introducing various substituted benzene ring in the main chain,[15] by using monomers containing certain heterocyclic units such as thiophene,[16,17] phenylquinoxaline ring,[18] or monomers with cardo-structure,[19] tetraphenylethene,[20] and others.[21] The motivation to prepare these poly-

Correspondence to: G.-S. Liou (E-mail: gsliou@ncnu.edu.tw)

Journal of Polymer Science: Part A: Polymer Chemistry, Vol. 45, 4921–4932 (2007)

mers was its potential application in photonic devices as thin films that could be cast from solutions. PAMs made by vapor deposition of the monomers in a vacuum chamber have also been used as electron transporting layers in polymer light-emitting diodes.[22,23]

The electroactive site of triphenylamine (TPA) is the nitrogen center, which is linked to three phenyl groups in a propeller-like geometry. The anodic oxidation pathway of TPA was well reported and the electrogenerated TPA cation radical dimerized to form tetraphenylbenzidine, which is more easily oxidized than the TPA molecule.[24–27] To obtain high T_g polymers, many investigators have prepared polymers containing TPA units in the main chain. Ogino et al. have successfully prepared TPA-containing polymers which had hole-transporting ability.[28,29] Murofushi et al. have also prepared a series of polytriphenylamines by carrying out Grignard reaction and then polymerizing the obtained Grignard reagent by using a nickel compound catalyst.[30,31] Recently, we have reported the synthesis of soluble aromatic poly(amine-amide)s,[32–35] poly (amine-imides)s,[33,36,37] and poly(amine hydrazide)s[38–40] bearing TPA units in the main chain. Because of the incorporation of bulky, three-dimensional TPA units along the polymer backbone, all the polymers were amorphous with good solubility in many aprotic solvents and exhibited excellent thin-film-forming capability.

Polymeric materials applied in thin layer electro-optical devices should exhibit reasonable electronic conductivity and proper band-gap energies or light absorption/emission in the desired region of the electromagnetic spectrum. For example, low band-gap polymers with absorption bands in the near-infrared region can be obtained by maximizing the π-electron delocalization within the conjugated polymer backbone through aromatic and quinoid type structures adopting coplanar conformations between the consecutive repeating units of polymer. A strategy employed in designing polymeric structures with desired electronic properties involves the synthesis of the donor–acceptor (D–A) type compound in which the D and A units are strong electron-donating (D) and electron-withdrawing (A) moieties, respectively.[41–47,49] Making appropriate choices for the D and A units allows one to control of the π-system's HOMO and LUMO energy levels. Therefore, the properties such as redox behavior and photophysical characteristics of the polymers can be tailored. In addition, because of the electronic nature of D–A polymers, they are able to show two different redox processes (oxidation and reduction), depending on which moiety (D or A) is involved.

In this article, we report the synthesis, characteristic, photophysical, and electrochemical studies of a new D–A chromophore system PAMs (Scheme 1). This molecule is basically a D–A type chromophore in which the electron-donating (D) moiety is a TPA group and the electron-withdrawing (A) moiety is a nitro group.

EXPERIMENTAL

Materials

Diphenylamine (Acros), 4-fluoronitrobenzene (Aldrich), sodium hydride (Aldrich), phosphorus oxychloride (Freak), 1,2-dichloroethane (TEDIA), *N*,*N*-dimethylformamide (DMF; Acros), *N*-methyl-2-pyrrolidinone (NMP; TEDIA), *N*,*N*-dimethylacetamide (DMAc; TEDIA), *m*-Cresol (Aldrich), chloroform ($CHCl_3$; TEDIA), tetrahydrofuran (THF; TEDIA), and methanol (Aldrich) were used without further purification. According to well-known chemistry, *N*-(4-nitrophenyl)-diphenylamine (**1**; mp = 144–145 °C) was synthesized by the nucleophilic fluoro-displacement reaction of 4-fluoronitrobenzene with diphenylamine.[36] 9,9-Bis(4-aminophenyl)fluorene (**3a**) (TCI) was obtained commercially and purified by sublimation. 4,4′-oxydianiline (**3b**) (TCI) was purchased and used as received. 4,4′-Diaminotriphenylamine (**3c**; mp = 186–187 °C) was synthesized by hydrazine Pd/C-catalyzed reduction of 4,4′-dinitrotriphenylamine resulting from the condensation of aniline with 4-fluoronitrobezene in the presence of cesium fluoride according to a previously reported procedure.[44] The aromatic diamines having bulky pendent triphenylamine group, *N*,*N*-bis(4-aminophenyl)-*N*′,*N*′-diphenyl-1,4-phenylenediamine[36] (**3d**; mp = 245–247 °C), and *N*,*N*-bis(4-aminophenyl)-*N*′,*N*′-diphenyl-1,2-phenylenediamine[33] (**3e**; mp = 219–222 °C) were prepared by the amination reaction of 4-aminotriphenylamine and 2-aminotriphenylamine with 4-fluoronitrobenzene, respectively, followed by hydrazine Pd/C-catalytic reduction. Tetrabutylammonium perchlorate (TBAP) was obtained from Acros and recrystallized twice from ethyl acetate and then dried *in vacuo* prior to use. All other reagents were used as received from commercial sources.

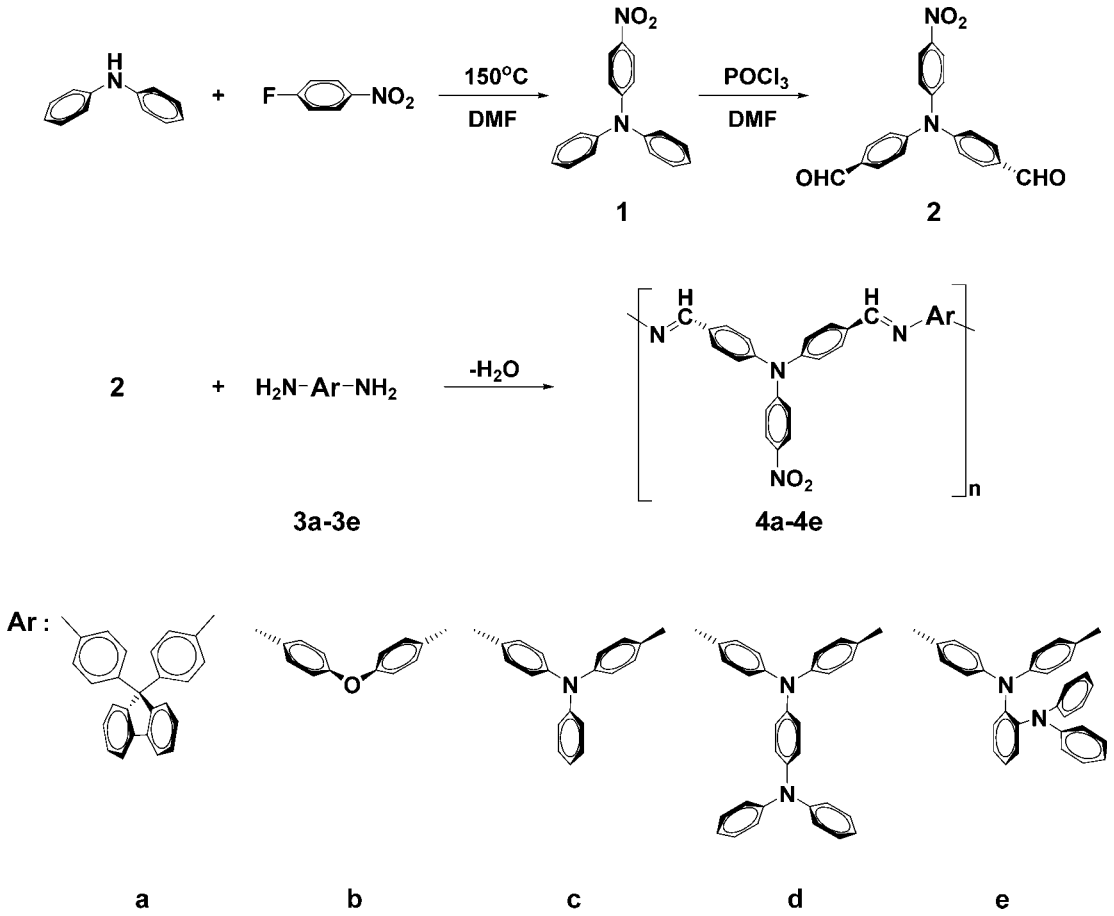

Scheme 1. Synthesis of donor-acceptor triphenylamine-based poly(azomethine)s.

Preparation of *N*-(4-nitrophenyl)-4′, 4″-bisformyl-diphenylamine

To 60 mL of DMF (0.78 mol) cooled at 0 °C in an ice bath, 56 mL of phosphorus oxychloride (0.60 mol) was added dropwise. The orange-yellow solution was allowed to warm up to room temperature with stirring. A solution of **1** (9.29 g, 0.032 mol) in 1,2-dichloroethane (400 mL) was added to the mixture at 35 °C. The reaction mixture was heated to reflux for 48 h, the resulting black mixture was trickled into cool water slowly with stirring and then extracted with chloroform. The combined chloroform solution was washed with water and dried over anhydrous $MgSO_4$. After removal of the solvent, a light-yellow product was recrystallized with acetone/hexane and afforded the dialdehyde monomer (6.03g, 54%), mp = 165–171 °C. FTIR (KBr): 2966 (aldehyde C—H stretch), 1698 (aldehyde C=O stretch), 1582, 1318 cm^{-1} (NO_2 stretch). FAB MS: *m/e* 346 (M^+). ^1H NMR ($CDCl_3$) δ 8.44 (s, 2H), 8.14–8.10 (d, 2H), 7.84–7.80 (d, 4H), 7.24–7.20 (d, 4H), 7.17–7.13 (d, 2H). ^{13}C NMR ($CDCl_3$) 190.47, 152.25, 151.44, 145.09, 131.87, 131.32, 127.09, 125.39, and 121.48.

Preparation of PAM 4a from 3a and 2

Into a flask fitted with a magnetic stirrer, were placed 0.523 g (1.5 mmol) of diamine **3a** and 3 mL of NMP. To the solution was added 0.520 g (1.5 mmol) of dialdehyde monomer **2**, and the solution was stirred at room temperature for 24 h under reduced pressure (0.1 torr). The polymer solution was filtered and cast onto a glass plate, then dried at 150 °C overnight under vacuum to prepare film. The yield was 0.979 g (99%). IR (KBr): 1674 cm^{-1} (C=N). ^1H NMR ($CDCl_3$) δ 8.42 (s, 2H), 8.13–8.12 (d, 2H), 7.85–7.80 (q, 6H), 7.45–7.35 (t, 2H), 7.32–7.15 (m, 12H), 7.12–7.00

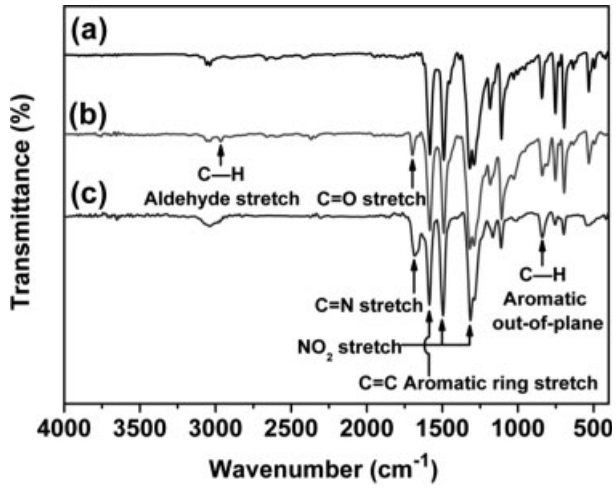

Figure 1. IR spectra of (a) compound 1, (b) compound 2, and (c) PAM **3c**.

(q, 6H). ^{13}C NMR ($CDCl_3$) 173.64, 158.09, 155.72, 152.81, 148.49, 147.21, 145.39, 141.13, 133.02, 132.71, 130.11, 126.76, 126.18, 125.43, 125.08, 122.30, 119.94, 119.43, and 49.41.

Additional NMR data of **PAM 4c**: ^{1}H NMR ($CDCl_3$) δ 8.44 (s, 2H), 8.05–8.02 (d, 2H), 7.86–7.81 (q, 4H), 7.40–7.34 (t, 2H), 7.22–6.89 (m, 17H). ^{13}C NMR ($CDCl_3$) 157.19, 156.34, 152.77, 147.97, 145.28, 140.91, 133.08, 132.86, 130.06, 129.92, 126.70, 125.35, 125.06, 124.52, 122.49, 119.76, and 119.65.

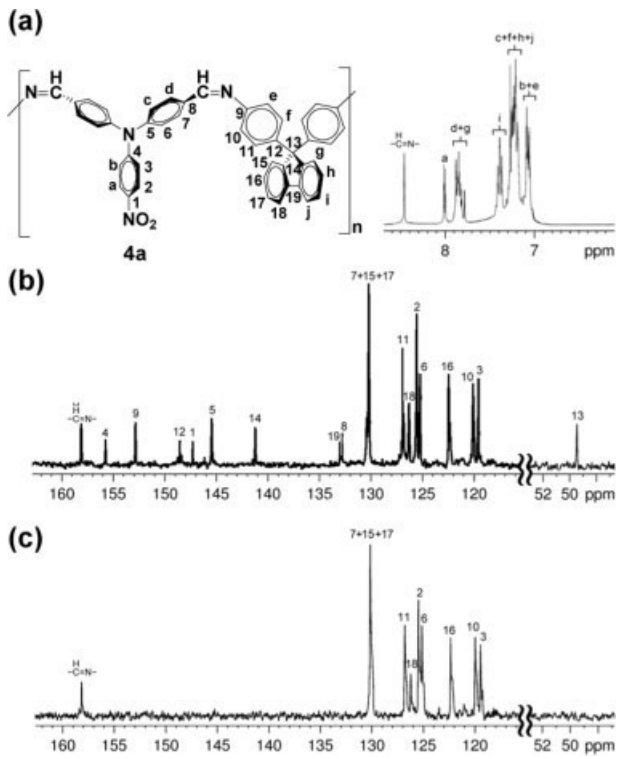

Figure 2. (a) ^{1}H NMR, (b) ^{13}C NMR, and (c) DEPT 135 spectra of PAM **4a** in CDCl.

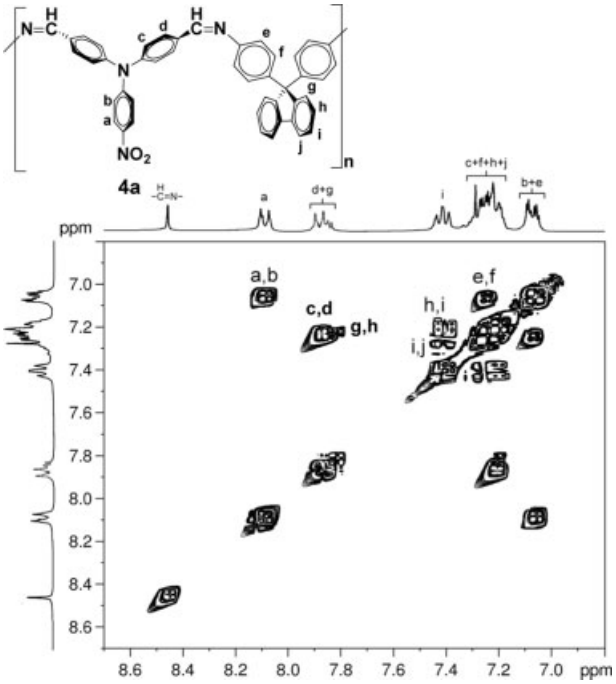

Figure 3. 2D ^{1}H-^{1}H correlated NMR spectroscopy (COSY) spectrum of PAM **4a** in $CDCl_3$.

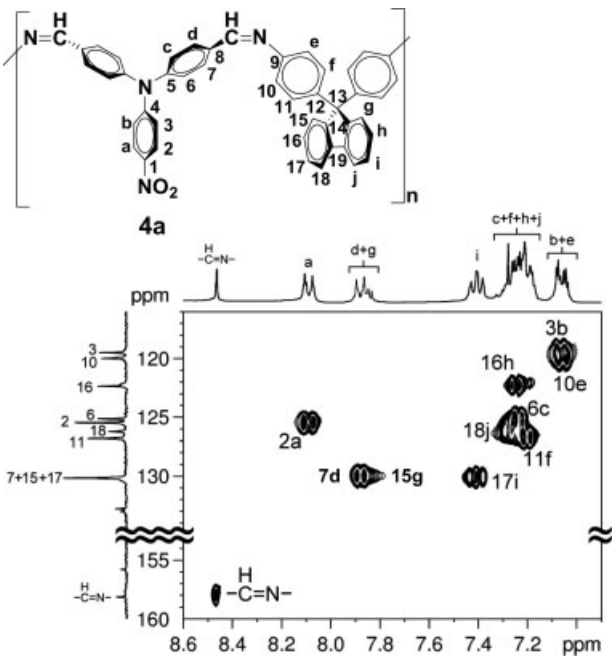

Figure 4. 2D ^{13}C-^{1}H heteronuclear multiquantum correlated NMR spectroscopy (HMQC) spectrum of PAM **4a** in $CDCl_3$.

Table 1. Molecular Weights and Thermal Properties of the Poly(azomethine)s

Polymer Code	Yield (%)	M_w[a]	PDI[b]	T_g (°C)[c]	T_d at 5% Weight loss (°C)[d]		T_d at 10% Weight Loss (°C)[d]		Char Yield (wt %)[e]
					N_2	Air	N_2	Air	
4a	99	7000	1.29	230	390	385	540	535	72
4b	97	6700	1.24	215	385	380	490	465	67
4c	95	10600	1.63	225	420	390	520	500	69
4d	93	9100	1.26	225	440	400	550	510	60
4e	98	8800	1.36	215	410	410	540	540	60

[a] Weight-average molecular weights relative to polystyrene standards in THF by GPC.
[b] PDI = M_w/M_n.
[c] Midpoint temperature of baseline shift on the DSC heating trace (rate 20 °C/min).
[d] Decomposition temperature, recorded via TGA at a heating rate of 20 °C/min and a gas-flow rate of 30 cm^3/min.
[e] Residual weight percentage at 800 °C in nitrogen.

Additional NMR data of **PAM 4d**: ^{1}H NMR ($CDCl_3$) δ 8.46 (s, 2H), 8.10–8.06 (d, 2H), 7.87–7.82 (q, 4H), 7.42–7.37 (t, 4H), 7.26–6.96 (m, 24H). ^{13}C NMR ($CDCl_3$) 157.10, 156.24, 152.87, 184.10, 146.15, 145.45, 141.95, 141.14, 133.26, 133.01, 130.12, 129.94, 126.18, 125.67, 125.46, 125.26, 125.18, 124.25, 122.57, 119.90, and 119.78.

Measurements

Infrared spectra were recorded on a PerkinElmer RXI FT-IR spectrometer. FAB-mass spectra were collected on a JMS-700 double focusing mass spectrometer (JEOL, Tokyo, Japan) with a resolution of 8000 (5% valley definition). For FAB-mass spectra, the source accelerating voltage was operated at 10 kV with a Xe gun, using 3-nitrobenzyl alcohol (NBA) as matrix. ^{1}H and ^{13}C NMR spectra were measured on a Bruker AV-300 FT-NMR system. Weight-average molecular weights (M_w) and number-average molecular weights (M_n) were obtained via size exclusion chromatography (SEC) on the basis of polystyrene calibration using a Water 2410 apparatus and tetrahydrofuran (THF) as the eluent. Ultraviolet-visible (UV-Vis) spectra of the sample were recorded on a Varian Cary 50 Probe spectrometer. Thermogravimetric analysis (TGA) was conducted with a PerkinElmer Pyris 1 TGA. Experiments were carried out on approximately 6 ~ 8 mg film samples heated in flowing nitrogen or air (flow rate = 20 cm^3/min) at a heating rate of 20 °C/min.

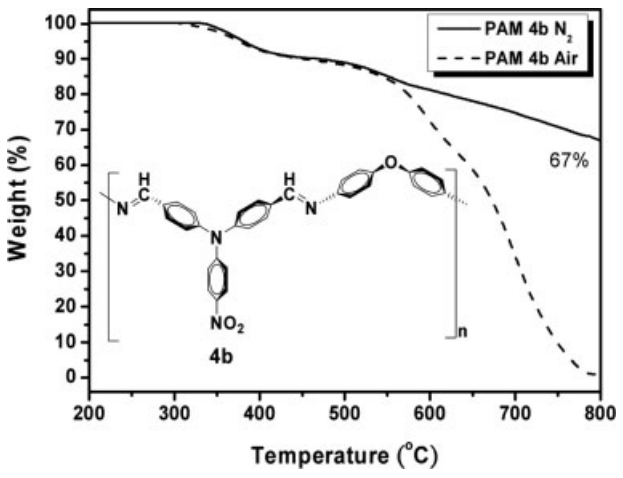

Figure 5. TGA thermograms of PAMs **4b** at a scanning rate of 20°C/min.

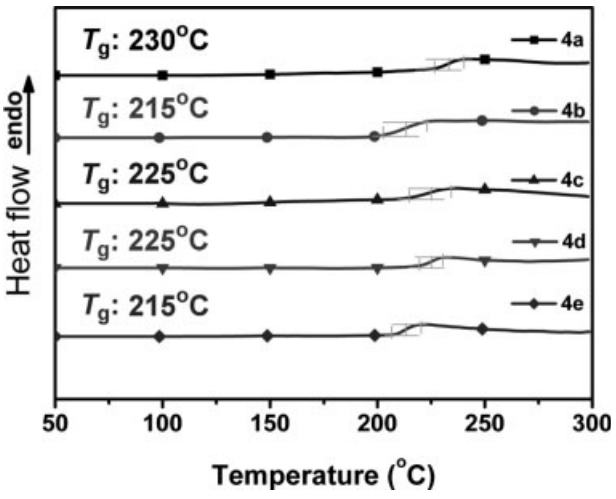

Figure 6. DSC curve for detection the glass transition temperatures (T_gs) of PAMS **4a–4e**.

Table 2. Photophysical Properties of the Poly(azomethine)s

	NMP (1×10^{-5} M) Solution, r.t.			Film, r.t.	
Polymer Code	λ_{abs} (nm)	λ_{em} (nm)	Φ_F (%)[b]	λ_{abs} (nm)	λ_{em} (nm)
4a	(262),405[a]	462	0.99	313,358,(418)[a]	550
4b	(263),410[a]	463	0.10	363,(417)[a]	516
4c	(262),416[a]	465	0.57	358,(418)[a]	542
4d	263,(319),415[a]	465	0.87	331,(418)[a]	561
4e	263,(292),421[a]	466	0.49	311,(415)[a]	549

[a] Excited wavelength.
[b] The value was measured by using 9,10-diphenylanthracene (dissolved in toluene with a concentration of 10^{-5} M, assuming fluorescence quantum efficiency of 0.90)[48] as a standard at 24–25 °C.

DSC analyses were performed on a PerkinElmer Pyris Diamond DSC at a scan rate of 20 °C/min in flowing nitrogen (20 cm^3/min). Electrochemistry was performed with a CHI 611B electrochemical analyzer. Voltammograms are presented with the positive potential pointing to the right and with increasing anodic currents pointing upwards. Cyclic voltammetry was conducted with the use of a three-electrode cell in which ITO (polymer films area about 0.7 cm × 0.5 cm) was used as a working electrode. A platinum wire was used as an auxiliary electrode. All cell potentials were taken with the use of a home-made Ag/AgCl reference electrode. Absorption spectra in spectroelectochemical analysis were measured with a HP 8453 UV-visible spectrophotometer. Photoluminescence spectra were measured with a Jasco FP-6300 spectrofluorometer.

RESULTS AND DISCUSSION

Synthesis and Characterization

Soluble aromatic poly(azomethine)s were prepared by the solution polycondensation of *N*-(4-nitrophenyl)-4′,4″-bisformyl-diphenylamine and aromatic diamines in *N*-methyl-2-pyrrolidone (NMP) at room temperature under reduced pressure. The synthesis route and structures of PAMs are shown in Scheme 1. The monomer compound **2**, *N*-(4-nitrophenyl)-4′,4″-bisformyl-diphenylamine, synthesized from *N*-(4-nitrophenyl)-diphenylamine by the Vilsmeier-Haack reaction is a blue light (462 nm) emitter with fluorescence quantum efficiency (Φ_F) of 1.10%.

The structures of monomer and polymer were confirmed by IR and NMR spectroscopy as shown in Figures 1–4. The IR spectrum of PAM **4c** showed a strong absorption band at 1684 cm^{-1},

Table 3. Electrochemical Properties of the Poly(azomethine)s

	Oxidation (V) (vs. Ag/AgCl)				Reduction (V) (vs. Ag/AgCl)				
Polymer Code	$E_{1/2}^{Ox,1}$ [a]	$E_{1/2}^{Ox,2}$ [a]	$E_{1/2}^{Ox,3}$ [a]	E_{onset}^{Ox} [b]	$E_{1/2}^{Re,1a}$	E_{onset}^{Re} [b]	E_{HOMO} (eV)[c]	E_{LUMO} (eV)[d]	E_g (eV)[e]
4a	1.24	–	–	1.09	−1.00	−0.98	5.43	3.34	2.09
4b	1.24	–	–	1.09	−1.00	−0.98	5.43	3.34	2.09
4c	1.11	1.29	–	1.00	−1.03	−1.00	5.34	3.31	2.03
4d	0.69	1.00	1.35	0.52	−1.03	−1.01	4.86	3.31	1.55
4e	0.87	1.03	1.29	0.76	−1.03	−1.01	5.10	3.31	1.79

[a] Half-wave potentials (V vs. Ag/AgCl) in CH_3CN containing 0.1 M TBAP.
[b] Onset potentials (V vs. Ag/AgCl) in CH_3CN containing 0.1 M TBAP.
[c] The HOMO energy levels were calculated from cyclic voltammetry and were referenced to ferrocene (4.8 eV).
[d] $E_{LUMO} = E_{HOMO} - E_g^{el}$.
[e] Electrochemical gap: $E_g^{el} = E_{onset}^{ox} - E_{onset}^{re}$.

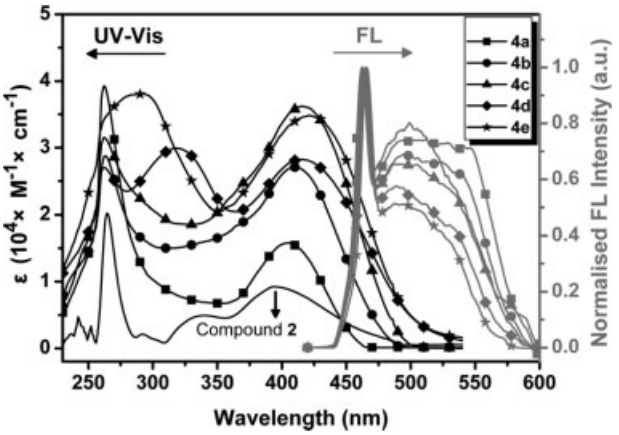

Figure 7. Molar absorptivity (left) and normalized fluorescence intensity (right) of compound 2 and PAMs **4a–4e** in NMP solution (ca. 1×10^{-5} M). a.u.: Arbitary units.

assigned to the azomethine (C=N) stretching. No clear signal for the amine end groups was detected above 3000 cm^{-1}. The ^1H NMR spectrum of PAM **4a** displayed a signal δ 9.92 which is attributed to the azomethine proton. The presence of a single signal for the azomethine proton suggested the occurrence of only one isomer, which is presumably the thermodynamically more stable trans-structure.

The introduction of TPA group is expected to increase solubility of the polymers. Thus, the resulting PAMs showed good solubility in common organic solvents, such as chloroform and THF. The molecular weight of PAMs **4a–4e** was measured by gel permeation chromatography (GPC), using polystyrenes as standard and THF as eluent. The weight-average molecular weight (M_w) and polydispersity (PDI) were determined as 6700–10,600 and 1.24–1.63, respectively (Table 1).

The PAMs **4a–4e** had useful levels of thermal stability, including 10% weight-loss temperatures beyond 490 °C (Fig. 5) and char yields at 800 °C in nitrogen higher than 60% associated with high glass transition temperatures (T_gs) (170–230 °C) (Fig. 6). The high char yields of the polymers can be ascribed to their high aromatic content. Physical properties of the polymer were investigated with spectroscopic, thermal analysis, and electrochemical studies (Tables 1–3).

Polymer Properties

Optical Properties

The optical properties of PAMs **4a–4e** were investigated by UV-Vis and fluorescence spectroscopy (Fig. 7). The main electronic absorptions are summarized in Table 2. All the PAMs in NMP solution showed π-π^* (nitro-substituted-TPA or K-band of aromatic azomethine unit) λ_{max} at 262–263 nm, and PAMs **4d** and **4e** exhibited additional n-π^* λ_{max} at 292–319 nm due to electron-donating TPA moieties from diamines **3d** and **3e**.

All the PAMs revealed CT absorptions at 405–421 nm. The colors of PAMs **4a–4e** films were from brownish to deep reddish that could be attributed to charge-transfer complex (CTC) for-

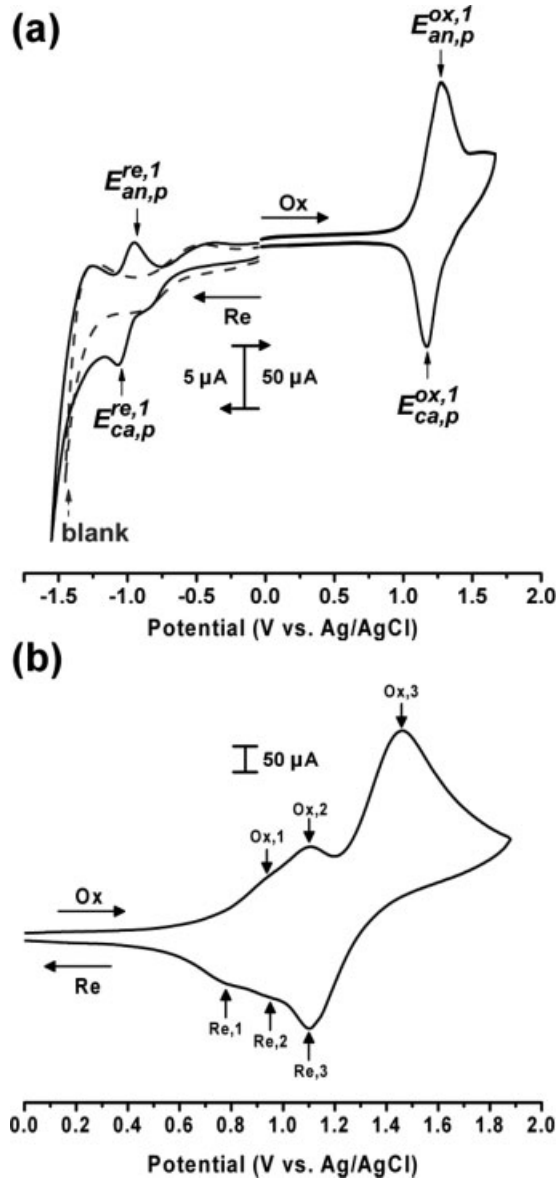

Figure 8. Cyclic voltammogram of (a) PAM 4b and (b) PAM **4e** films onto an indium-tin oxide (ITO) coated glass substrate in CH_3CN solution containing 0.1 M TBAP at scan rate = 0.1 V/s.

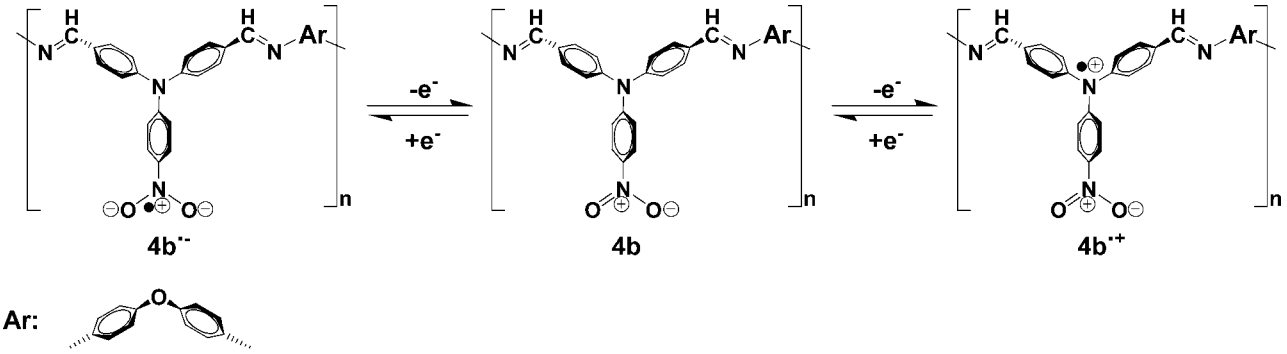

Scheme 2. Anodic oxidation and cathodic reduction pathways for PAM **4b**.

mation between the electron-donating TPA group and the strongly electron-accepting nitro group. The CT absorption of PAM **4a** is around 405 nm. PAMs **4d** and **4e** with higher electron-donating diamine structures also showed red shift absorptions of 10 and 16 nm, respectively. Besides, they exhibited a maximum blue fluorescence at 462–466 nm with fluorescence quantum efficiency (Φ_F) of 0.49–0.99% in NMP solution, and at 516–561 nm in film state with red shifts (53–96 nm) because of additional intermolecular CTC.

Electrochemical Properties

The electrochemical behaviors of the PAMs **4a–4e** were investigated with cyclic voltammetry conducted for the cast film on an ITO-coated glass substrate as working electrode in dry acetonitrile (CH_3CN) containing 0.1 M TBAP as an electrolyte under nitrogen atmosphere. PAMs **4a–4e** are all electrochemically stable polymers. Figure 8 shows a representative cyclic voltammogram of PAM **4b**, which exhibits a reversible oxidation and a reversible reduction. The anodic oxidation[45,50] and cathode reduction[51] pathway of PAM **4b** are postulated as shown in Scheme 2. The electrochemical oxidation and reduction potentials of the polymers are given in Table 3. The highest occupied molecular orbital (HOMO) and lowest unoccupied molecular orbital (LUMO) energy levels can be determined from the oxidation and reduction onset potentials of cyclic voltammetry as 4.86–5.43 and 3.31–3.34 eV, respectively.

For example (Fig. 8), the onset potentials (E_{onset}) of oxidation and reduction for PAM **4b** film are observed at +1.09 and −1.00 V, respectively, versus Ag/AgCl in CH_3CN, and the external ferrocene/ferrocenium (Fc/Fc^+) redox standard $E_{1/2}$ is 0.46 V. Assuming that the HOMO energy for the Fc/Fc^+ standard is 4.80 eV with respect to the zero vacuum level, the HOMO energy for PAM **4b** has been evaluated to be 5.43 eV. For PAM **4b**, the electrochemical gap (E_g^{el}, 2.09 eV) is the difference with the onset potential of oxidation and the onset potential of reduction. Therefore, the LUMO value (3.34 eV) could be obtained from electrochemical gap minus the HOMO value.

The effect of the HOMO value on the electrochemical gap is also shown in Table 3. Moreover, side-group substitution such as electron-donating group (e.g., *o*-TPA and *p*-TPA) also causes a difference in electrochemical behavior. The relation between energy band-gaps (E_g,:1.55–2.09 eV) and structures of PAMs **4a–4e** with different diamine moieties was investigated by electrochemical or optical absorption measurements, and the results are in good agreement as shown in Table 3.

Optimized Geometry Properties

Optimized geometry for PAM **4a–4e** was obtained by minimizing energy via semi-empirical Austin Model 1 (AM1) calculation in the gas state. AM1 is not only a semi-empirical self-consistent field (SCF) method for chemical calculations but also an improvement of the modified neglect of differential diatomic overlap (MNDO) method. Together with Parameterized Model number 3 (PM3), AM1 is generally the most accurate semi-empirical method and useful for molecules containing elements from long rows 1 and 2 of the periodic table. The molecular model was implemented in the Hyperchem molecular graphics package.[52]

Since each of 4-nitro-triphenylamine group is twisted from another TPA segment in PAMs **4c–4e** at 0.0–22.4°, it could be suggested that the twisted structure between repeat segments in

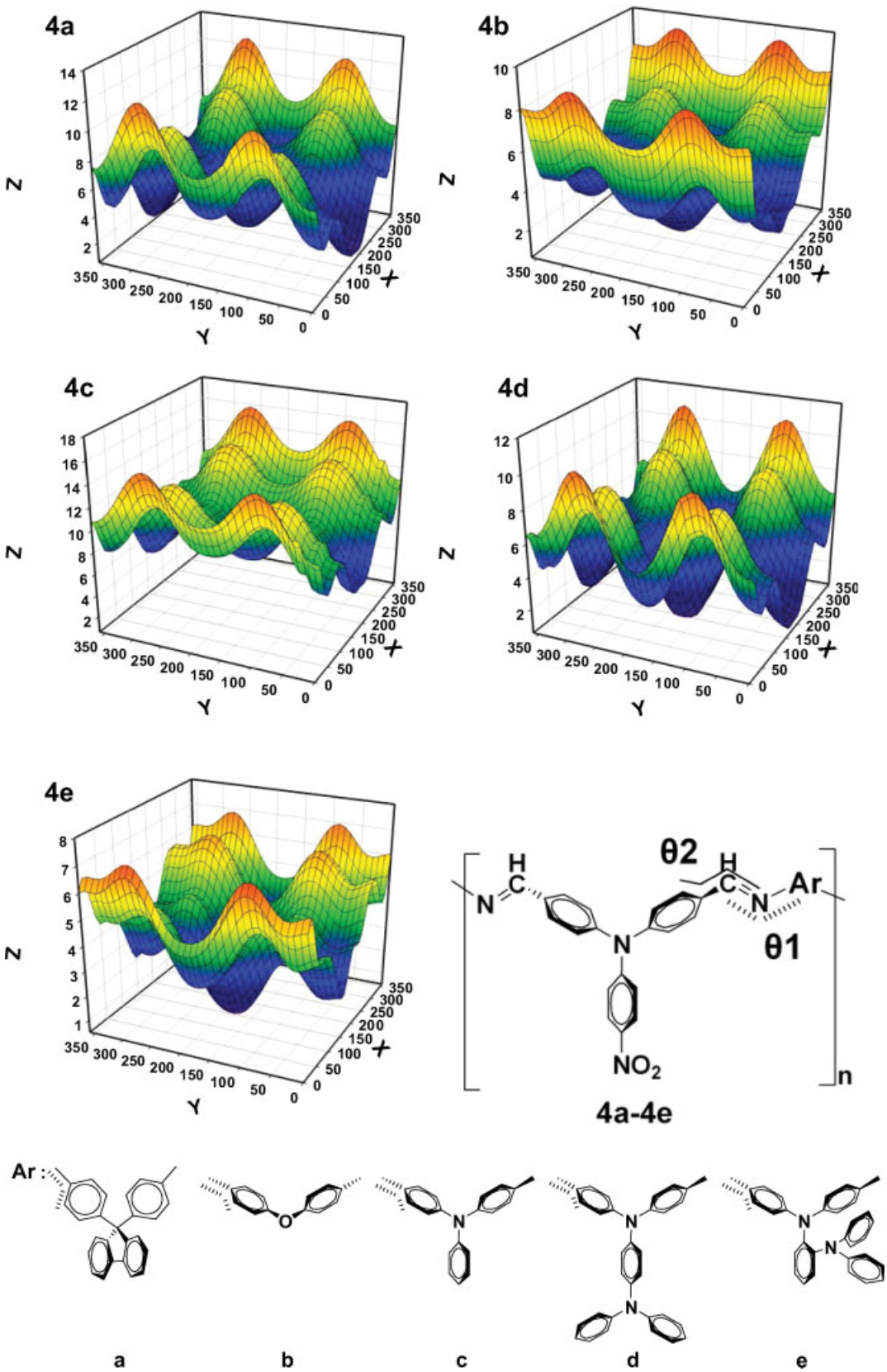

Figure 9. Potential energy surface and contour graph for PAMs **4a–4e** as a function of the dihedral $\theta 1$ (degree), Y axis: $\theta 2$ (degree), Z axis: Relative Energy (kcal/mol). [Color figure can be viewed in the online issue, which is available at www.interscience.wiley.com.]

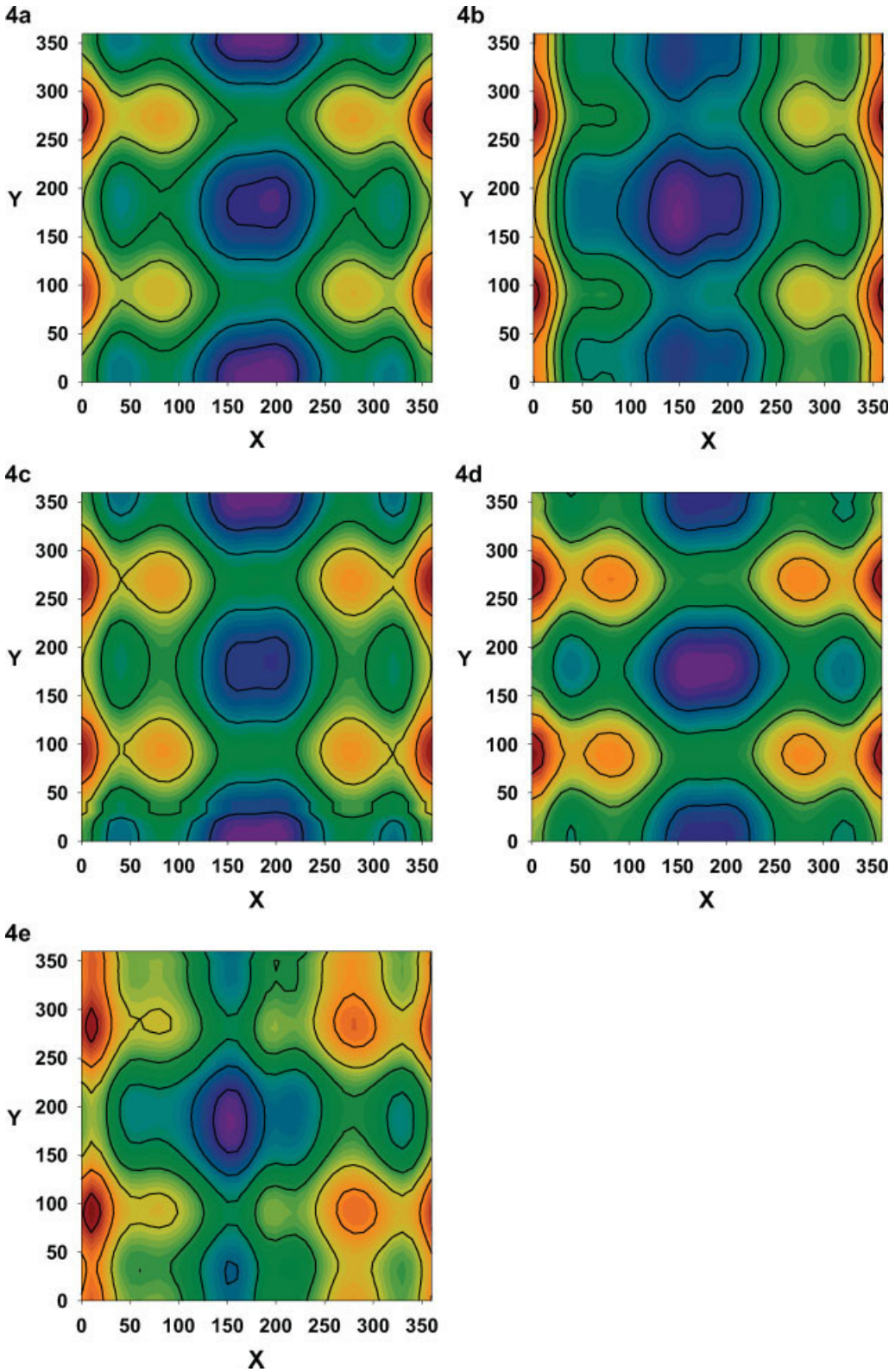

Figure 10. Contour graphs of potential energy surface for PAMs **4a–4e**. *X* axis: $\theta 1$ (degree). *Y* axis: $\theta 2$ (degree). [Color figure can be viewed in the online issue, which is available at www.interscience.wiley.com.]

PAMs **4c–4e** could not efficiently limit delocalization of electronic charges. Moreover, side-group substitution such as electron-donating group (e.g., *o*-TPA and *p*-TPA) also causes a lower reduction potential in electrochemical behavior as shown in Table 3. Therefore, the delocalized electron coupling can interpret intervalence charge-transfer (IV-CT) absorption spectra within two and/or three electoractive nitrogen redox centers between the TPA units of PAMs **4c–4e**, and show two and/or three different oxidation potentials from cyclic voltammetric scanning (Table 3).[53] Although only a single conformation is observed for the optimized molecular geometry of PAMs **4a–4e**, it is possible that the relaxation of packing constraints in solution might allow other conformations to be present.[54] Therefore, a molecular mechanic study was undertaken to determine the potential energy (in kcal/mol) of the molecule as a function of the dihedral angle $\theta 1$ or $\theta 2$, and the results are plotted in Figs. 9 and 10.

CONCLUSIONS

The synthetic pathways of a donor–acceptor (D–A) PAM system with low band-gap have been successfully established. The results presented herein demonstrated that incorporating bulky 4-nitro-TPA group into PAM backbone not only enhanced the solubility for processing but also revealed good thermal stability, stable electrochemical characteristic, higher HOMO and lower LUMO energy level. Thus, these donor–acceptor 4-nitro-TPA-containing PAMs may be widely applied in electric and optical devices as bipolar materials due to their proper HOMO and LUMO values, and excellent thermal stability.

The authors are grateful to the National Science Council of the Republic of China for financial support of this work.

REFERENCES AND NOTES

1. Yang, C.-J.; Jenekhe, S. A. Chem Mater 1991, 3, 878.
2. Spiliopoulos, I. K.; Mikroyannidis, J. A. Macromolecules 1996, 29, 5313.
3. Cerrada, P.; Oriol, L.; Piñol, M.; Serrano, J. L.; Iribarren, I.; Munoz Guerra, S. Macromolecules 1996, 29, 2515.
4. Kiriy, N.; Bocharova, V.; Kiriy, A.; Stamm, M.; Krebs, F. C.; Adler, H.-J. Chem Mater 2004, 16, 4765.
5. Zotti, G.; Randi, A.; Destri, S.; Porzio, W.; Schiavon, G. Chem Mater 2002, 14, 4550.
6. Tsai, F.-C.; Chang, C.-C.; Liu, C.-L.; Chen, W.-C.; Jenekhe, S. A. Macromolecules 2005, 38, 1958.
7. Liu, C.-L.; Tsai, F.-C.; Chang, C.-C.; Hsieh, K.-H.; Lin, J.-L.; Chen, W.-C. Polymer 2005, 46, 4950.
8. Liu, C.-L.; Chen W.-C. Macromol Chem Phys 2005, 206, 2212.
9. Kimoto, A.; Masachika, K.; Cho, J.-S.; Higuchi, M.; Yamamoto K. Chem Mater 2004, 16, 5706.
10. Choi, M. K.; Kim, H. L.; Suh, D. H. J Appl Polym Sci 2006, 101, 1228.
11. Cazacu, M.; Marcu, M.; Vlad, A.; Tóth, A.; Racles C. J Polym Sci Part A: Polym Chem 2003, 41, 3169.
12. Adell, J. M.; Alonso, M. P.; Barberá, J.; Oriol, L.; Piñol, M. Serrano J. L. Polymer 2003, 44, 7829.
13. Yang, H. H. Aromatic High Strength Fibers; Wiley: New York, 1989; pp 641–673.
14. Kricheldorf, H. R.; Schwarz, G. In Handbook of Polymer Synthesis, Part B; Kricheldorf, H. R.; ed. Dekker: New York, 1992; pp 1673–1684.
15. Yamamoto, T.; Zhou, Z.-H.; Kanbara, T.; Shimura, M.; Kizu, K.; Maruyama, T.; Nakamura, Y.; Fukuda, T.; Lee, B.-L.; Ooba, N.; Tomaru, S.; Kurihara, T.; Kaino, T.; Kubota, K.; Sasaki, S. J Am Chem Soc 1996, 118, 10389.
16. Wang, C.; Shieh, S.; LeGoff, E.; Kanatzidis, M. G. Macromolecules 1996, 29, 3147.
17. Olinga, T. E.; Destri, S.; Botta, C.; Porzio, W.; Consonni, R. Macromolecules 1998, 31, 1070.
18. Klein, D. J.; Modarelli, D. A.; Harris, F. W. Macromolecules 2001, 34, 2427.
19. Chiang, C.-L.; Shu C.-F. Chem Mater 2002, 14, 682.
20. Matsumoto, T.; Yamada, F.; Kurosaki, T. Macromolecules 1997, 30, 3547.
21. Giuseppone, N.; Fuks, G.; Lehn J.-M. Chem Eur J 2006, 12, 1723.
22. Fischer, W.; Stelzer, F.; Meghdadi, F.; Leising, G. Synth Met 1996, 76, 201.
23. Weaver, M. S.; Bradley, D. D. C. Synth Met 1996, 83, 61.
24. Zhang, T.; Brajter-Toth, A. Anal Chem 2000, 72, 2533.
25. Oyama, M.; Nozaki, K.; Okazaki, S. Anal Chem 1991, 63, 1387.
26. Creason, S. C.; Wheeler, J.; Nelson, R. F. J Org Chem 1972, 37, 4440.
27. Seo, E. T.; Nelson, R. F.; Fritsch, J. M.; Marcoux, L. S.; Leedy, D. W.; Adams, R. N. J Am Chem Soc 1966, 88, 3498.
28. Son, J. M.; Mori, T.; Ogino, K.; Sato, H.; Ito, Y. Macromolecules 1999, 32, 4849.
29. Ogino, K.; Kanegae, A.; Yamaguchi, R.; Sato, H.; Kurjata, J. Macromol Rapid Commun 1999, 20, 103.
30. Ohsawa, Y.; Ishikawa, M.; Miyamoto, T.; Murofushi, Y.; Kawai, M. Synthetic Metals 1987, 18, 371.

31. Ishikawa, M.; Kawai, M.; Ohsawa, Y. Synthetic Metals 1991, 40, 231.
32. Liou, G.-S.; Hsiao, S.-H.; Huang, N.-K.; Yang, Y.-L. Macromolecules 2006, 39, 5337.
33. Liou, G.-S.; Yang, Y.-L.; Su, Y. O. J Polym Sci Part A: Polym Chem 2006, 44, 2587.
34. Liou, G.-S.; Huang, N.-K.; Yang, Y.-L. J Polym Sci Part A: Polym Chem 2006, 44, 4095.
35. Liou, G.-S.; Huang, N.-K.; Yang, Y.-L. Polymer 2006, 47, 7013.
36. Cheng, S.-H.; Hsiao, S.-H.; Su, T.-H.; Liou, G.-S. Macromolecules 2005, 38, 307.
37. Hsiao, S.-H.; Chang, Y.-M.; Chen, H.-W.; Liou, G.-S. J Polym Sci Part A: Polym Chem 2006, 44, 4579.
38. Liou, G.-S.; Hsiao, S.-H.; Chen, W.-C.; Yen, H.-J. Macromolecules 2006, 39, 6036.
39. Liou, G.-S.; Huang, N.-K.; Yang, Y.-L. J Polym Sci Part A: Polym Chem 2007, 45, 48.
40. Liou, G.-S.; Huang, N.-K.; Yang, Y.-L. Eur Polym J 2006, 42, 2283.
41. Roncali, J. Chem Rev 1997, 97, 173.
42. Zhang, Q. T.; Tour, J. M. J Am Chem Soc 1998, 120, 5355.
43. Devasagayaraj, A.; Tour, J. M. Macromolecules 1999, 32, 6425.
44. Oishi, Y.; Ishida, M.; Kakimoto, M.; Imai, Y.; Kurosaki, T. J Polym Sci Part A: Polym Chem 1992, 30, 1027.
45. Chiu, K.-Y.; Su, T.-X.; Li, J.-H.; Lin, T.-H.; Liou, G.-S.; Cheng S.-H. J Electroanal Chem 2005, 575, 95.
46. Kim, Y.-H.; Zhao, Q.; Kwon, S.-K. J Polym Sci Part A: Polym Chem 2006, 44, 172.
47. Barberis, V. P.; Mikroyannidis, J. A. J Polym Sci Part A: Polym Chem 2006, 44, 3556.
48. Hamai, S.; Hirayama, F. J Phys Chem 1983, 87, 83.
49. Lim, E.; Jung, B.-J.; Shim, H.-K. J Polym Sci Part A: Polym Chem 2006, 44, 243.
50. Yeh, S.-J.; Tsai, C.-Y.; Huang, C.-Y.; Liou, G.-S.; Cheng, S.-H. Electrochem Commun 2003, 5, 373.
51. Zhao, Y.; Bordwell, F. G. J Org Chem 1996, 61, 6623.
52. Hyperchem Vers. 7.5; Hypercube: Hypercube, Inc., Gainesville, FL., 2003.
53. Lambert, C.; Nöll, G. J Am Chem Soc 2005, 121, 8434.
54. Woolft, T. B.; Roux B. J Am Chem Soc 1994, 116, 5916.